Effect of Ni addition on microstructure, mechanical and high temperature behavior of mechanically alloyed W-Nb

P. Meher[1], C. Kiran[1], **A. Patra[1*]**, R. Saxena[1], S. K. Karak[1]

[1]*Nanomaterials Research Group, Metallurgical and Materials Engineering Department,*

National Institute of Technology Rourkela, Rourkela-769008, Odisha, India.

*Corresponding Author E-mail: *patraa@nitrkl.ac.in*

ABSTRACT

The present investigation comprises the fabrication of tungsten (W) based alloys with nominal composition of $W_{70}Ni_{20}Nb_{10}$ (alloy A), $W_{75}Ni_{15}Nb_{10}$, (alloy B) (all in wt.%) by mechanical alloying (MA) in a planetary ball mill followed by sintering at 1500°C for 2 h in Ar atmosphere. The milled powders and the consolidated products have been investigated by X-ray diffraction (XRD), Scanning electron microscopy (SEM) and energy dispersive spectroscopy (EDS). Minimum crystallite size and maximum lattice strain of 45 nm and 0.42% respectively is achieved in alloy B. Maximum sinterability, hardness of 90.5%, 4.58 GPa (at 50g) respectively is achieved in alloy B due to finer crystallite size, higher surface energy and shorter atomic diffusion distance whereas maximum compressive strength of 2.14 GPa and minimum wear rate is achieved in alloy A owing to the formation of higher fraction of hard NbNi intermetallic phase. High temperature oxidation study at 900°C for 10 h reveals that lower oxidation rate is achieved in alloy A owing to lesser weight fraction of W and higher propensity of protective $NiWO_4$ scale formation.

Keywords: W based alloy; Mechanical alloying; Strength; Oxidation.

Effect of Ni addition on microstructure, mechanical and high temperature behavior of mechanically alloyed W-Nb

International Conference on Nanotechnology : Ideas, Innovations & Initiativies-2017 (ICN: 3I-2017)
IIT Roorkee
8th December, 2017

P. Meher, C. Kiran, A. Patra*, R. Saxena, S. K. Karak

Department of Metallurgical and Materials Engineering

NATIONAL INSTITUTE OF TECHNOLOGY, ROURKELA
ROURKELA-769008, INDIA

BRIEF OUTLINE

- Aims and Objective
- Introduction & Background
- Materials and Method
- Result & Discussions
- Conclusions
- References

Aims and Objective

- To fabricate W based alloys through pressure less **liquid phase sintering**.

- Investigate the physical, mechanical and high temperature behavior of the fabricated alloys.

Introduction & Background

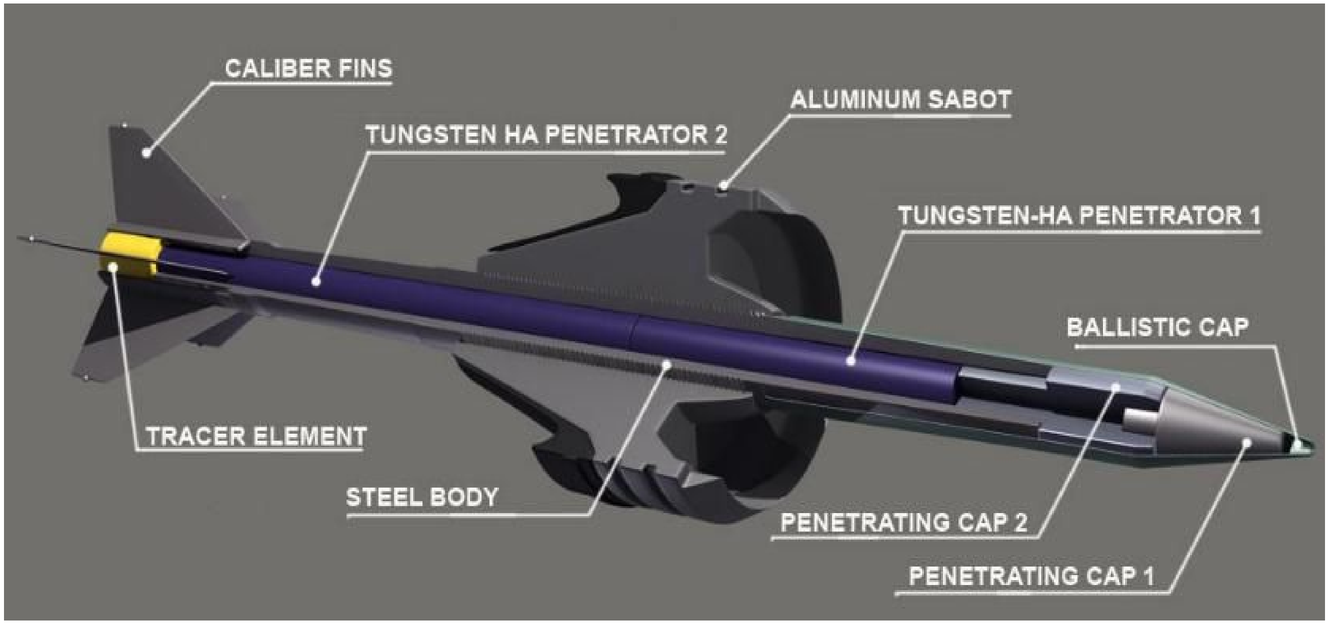

- **Extreme temperature (~1000-1500°C)**
- **High strain rate (10^6 s^{-1}) and**
- **Hydrostatic pressure (2–6 GPa)**

A. Upadhyaya, Mater. Chem. Phys. 67 (2001) 101–110.

Introduction & Background

➢Any other application?

1. Radiation Shielding
2. Aviation counterweights
3. High rigidity tooling components

Die & Punch

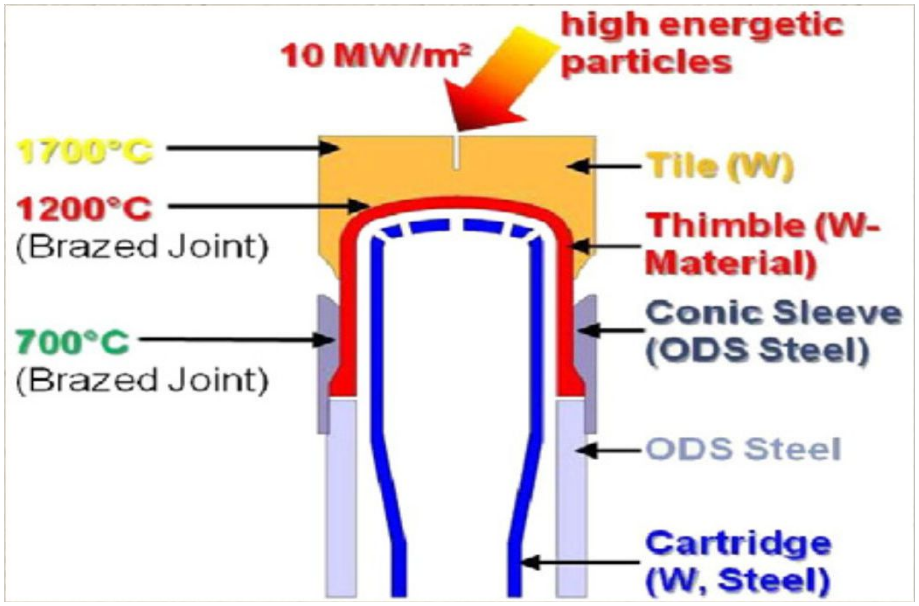

Radiation Shielding

Aviation counterweights

Introduction & Background

➢Why Tungsten?

Pros..

- High Melting point (3420^0C).
- High hardness (9.8 GPa), MOE=407 GPa.
- Good thermal conductivity (1.74 W/cm K) , low co-efficient of thermal expansion.
- Low-activating metal in radiation environment with low sputtering yield.

(W.F. Smith, McGraw-Hill, 1993)

➢Cons.. with Tungsten

High ductile brittle transition temperature (200-500°C).

(J. L. Johnson, Sintering of refractory metals, Woodhead Publishing, Cambridge (UK) 2010, pp. 357–380).

Introduction & Background

➢Why alloy addition ?

- To Improve fabricability and effective utilization of Tungsten.
- Ni imparts liquid phase sintering (if sintering temp is higher than m.p. of Ni) and improve plastic flow properties.
- To improve the high temperature strength and lower the DBTT of W by Nb addition.

A. Patra et al. , Int. J. Refract. Met. Hard Mater 60 (2016) 131–146

Introduction & Background

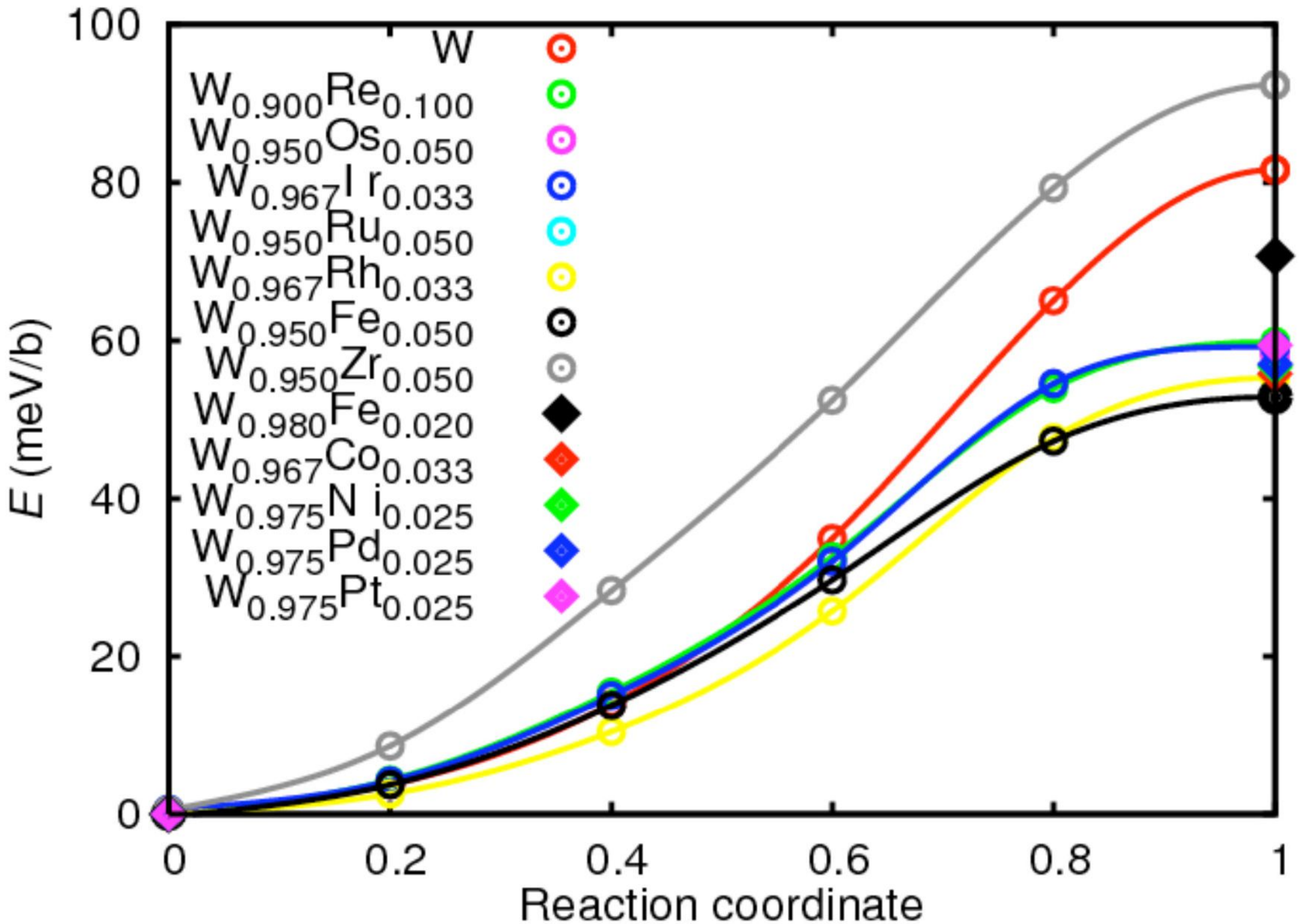

G. D. Samolyuk et. al Fusion Reactor Materials Program (2011)

Introduction & Background

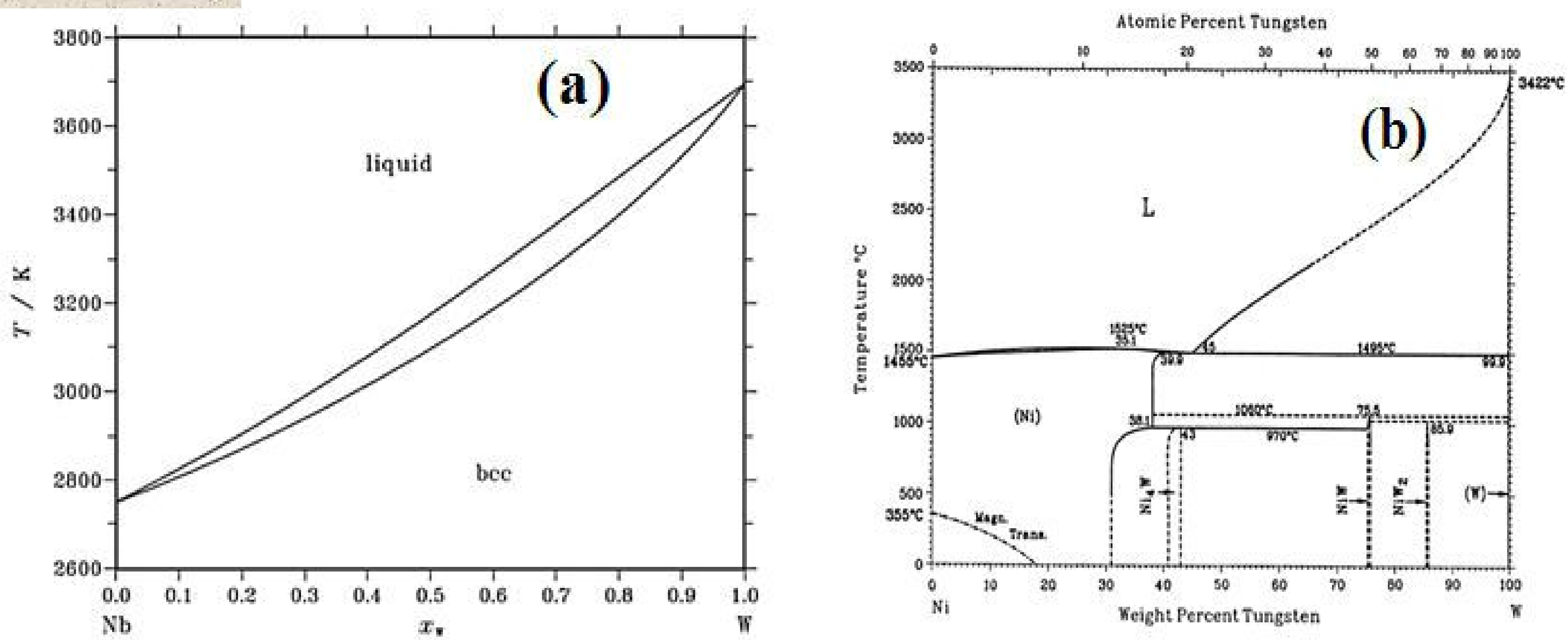

Binary alloy phase diagrams of (a) W-Nb [P. Franke et al. 2006], (b) W-Ni [T. B. Massalski et al. 1990]

Introduction & Background

➢Why Nanostructuring ?

- To lower the sintering temperature.
  (R malewar *et.al, J. Mater. Res., 22 (2007*)

- To improve the mechanical properties.
  [H. Glieter, *Acta. Mater.*, 48 (2000)]

Materials & Methods

Elemental powders (W, Ni, Nb)

↓

High Energy Ball-Mill (20 h)

↓

Nanostructured Alloy Powder

↓

Characterization
(XRD, SEM)

↓

Pressureless sintering (1500°C, 2 h holding)

↓

Characterization
[XRD, SEM, Density, Hardness, Strength, Wear, Oxidation]

Materials & Methods

Mechanical Alloying

Mechanism of MA

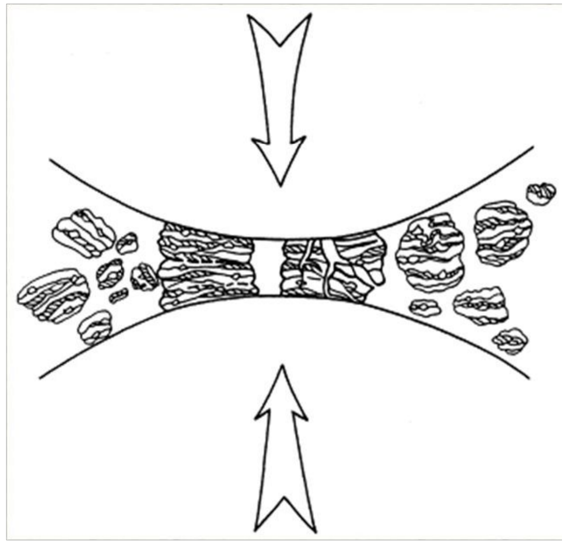

- **Elemental powders of W, Ni, Nb (purity 99.5%, Sigma Aldrich) initial particle of 100-150 µm**

Alloy	Composition (wt.%)		
	W	Ni	Nb
Alloy A	70	20	10
Alloy B	75	15	10

- **FRISTSCH planetary ball mill, steel vials and 10 mm chrome steel balls**
- **300 rpm, 10:1 (ball to powder weight). Wet milling with toluene (Process control agent to prevent particle agglomeration)**

Materials & Methods

Compaction
500 MPa pressure
5 min dwell time

(a) Conventional Sintering Furnace (1500°C for 2 h) (Ar flow rate : 100 ml/min)

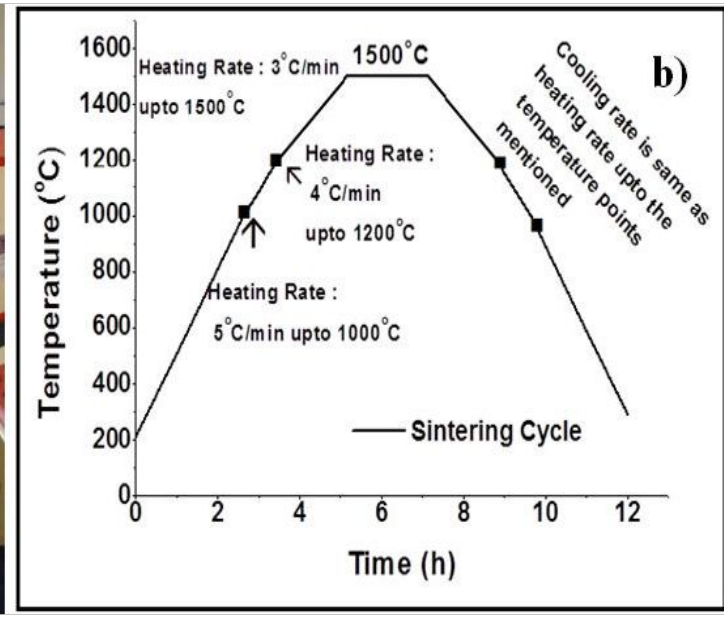

(b) Conventional Sintering Cycle

Results and discussion

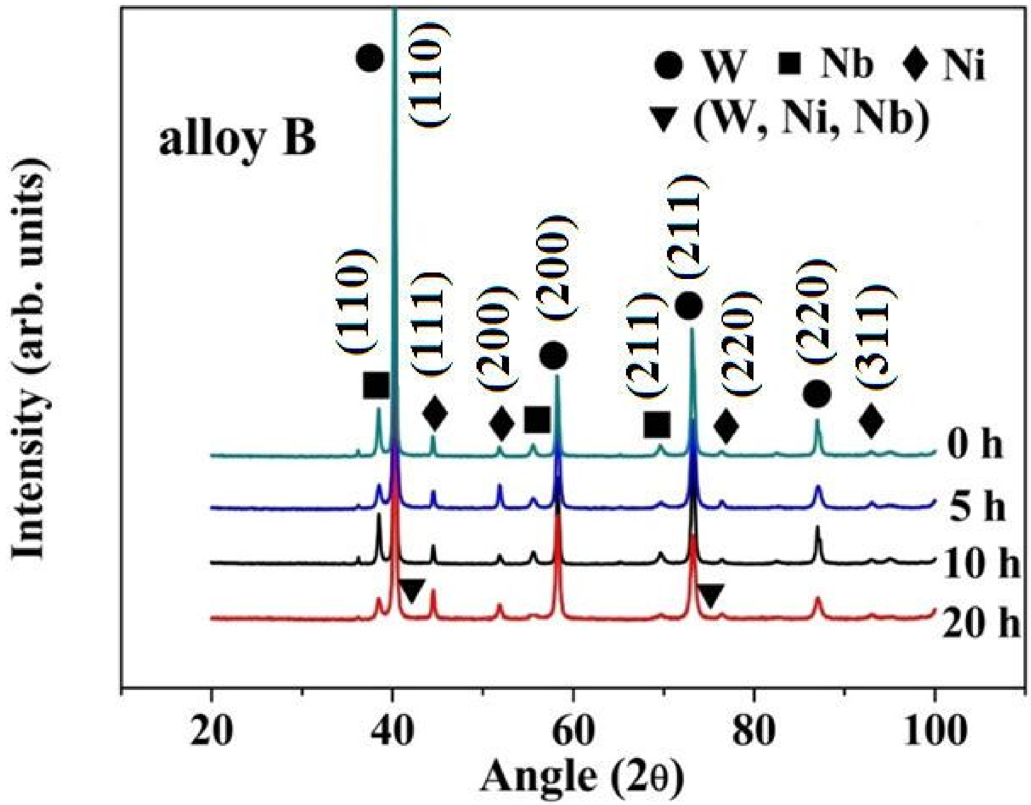

XRD pattern of alloy B mechanically alloyed at various time (0, 5, 10, 20 h).

- W and Nb : unlimited solid solubility (similar crystal structure (BCC) and small difference between atomic radius (W: 193 pm, Nb: 198 pm)

- W and Ni : limited solid solubility (different crystal structure (Ni : FCC) and wide difference between atomic radius (W: 193 pm, Ni: 149 pm)

Results and discussion

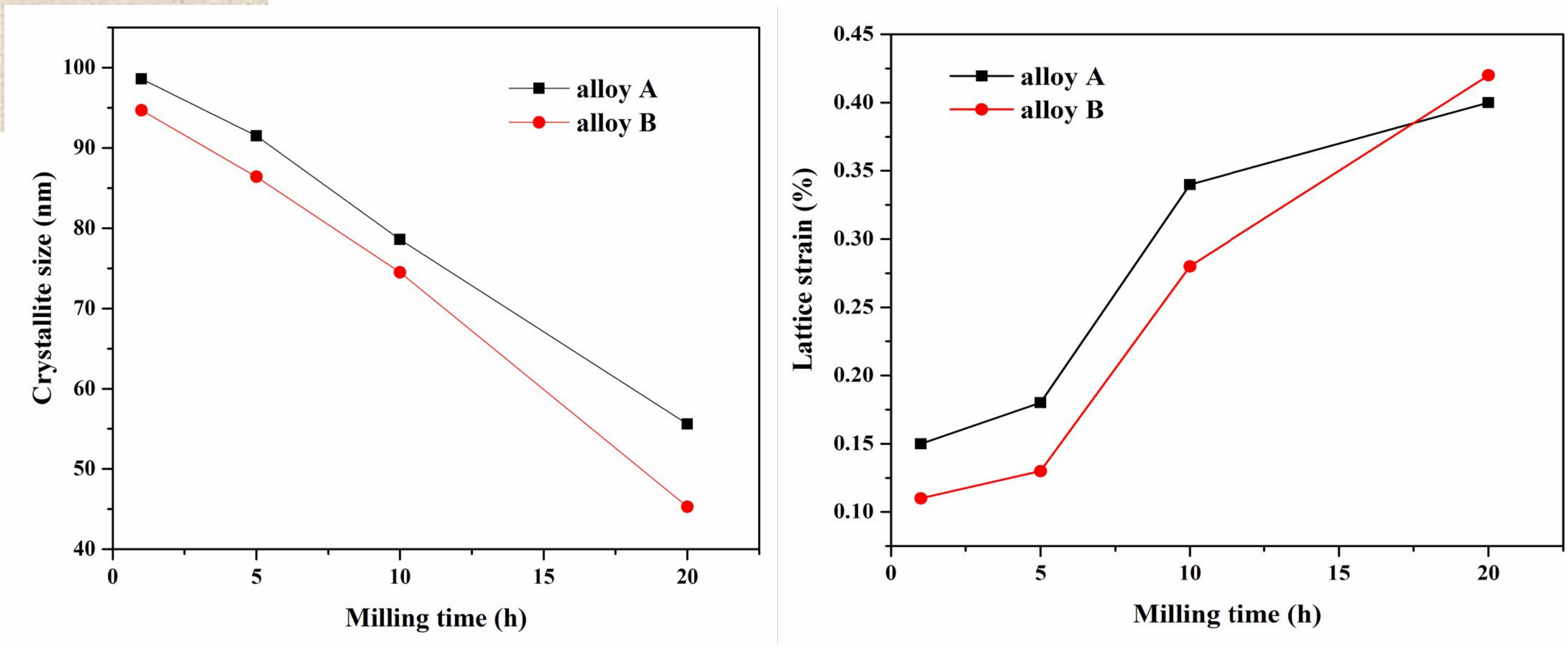

Variation of crystallite size and lattice strain of alloy A and alloy B with milling time

$$\beta \cos\theta = \frac{0.94\lambda}{D} + 4\eta \sin\theta,$$

where, β is the full width half maxima (FWHM), D is the crystallite size and η is the lattice strain.

Results and discussion

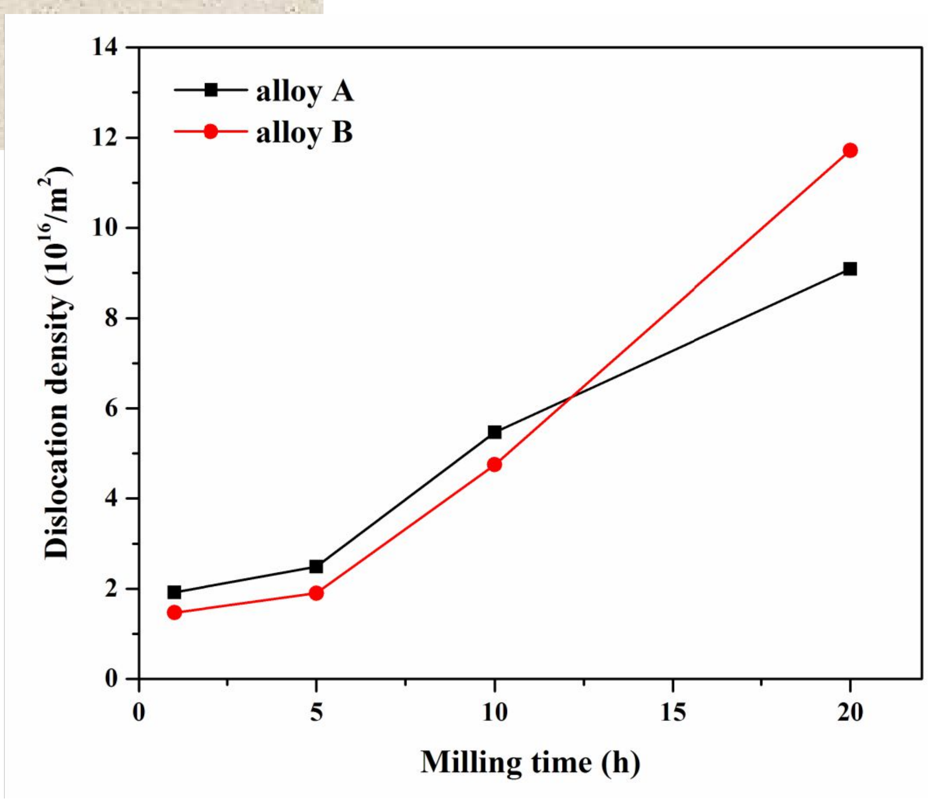

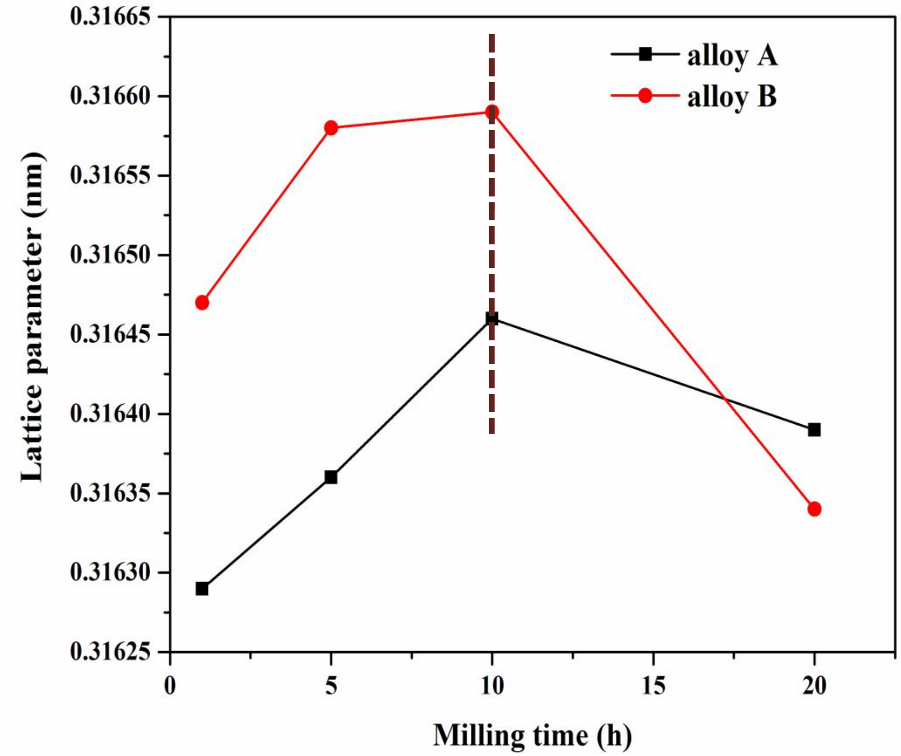

$$\rho_d = 2\sqrt{3}\,\frac{\left(\varepsilon^2\right)^{1/2}}{D \times b}$$

b is the burgers vector of dislocations, b = (a√3)/2 for the bcc structure, a= cell parameter = lattice parameter, D = crystallite size, ε = lattice strain

Y. H. Zhao, Acta Mater. 49 (2) (2001) 365–375

Results and discussion

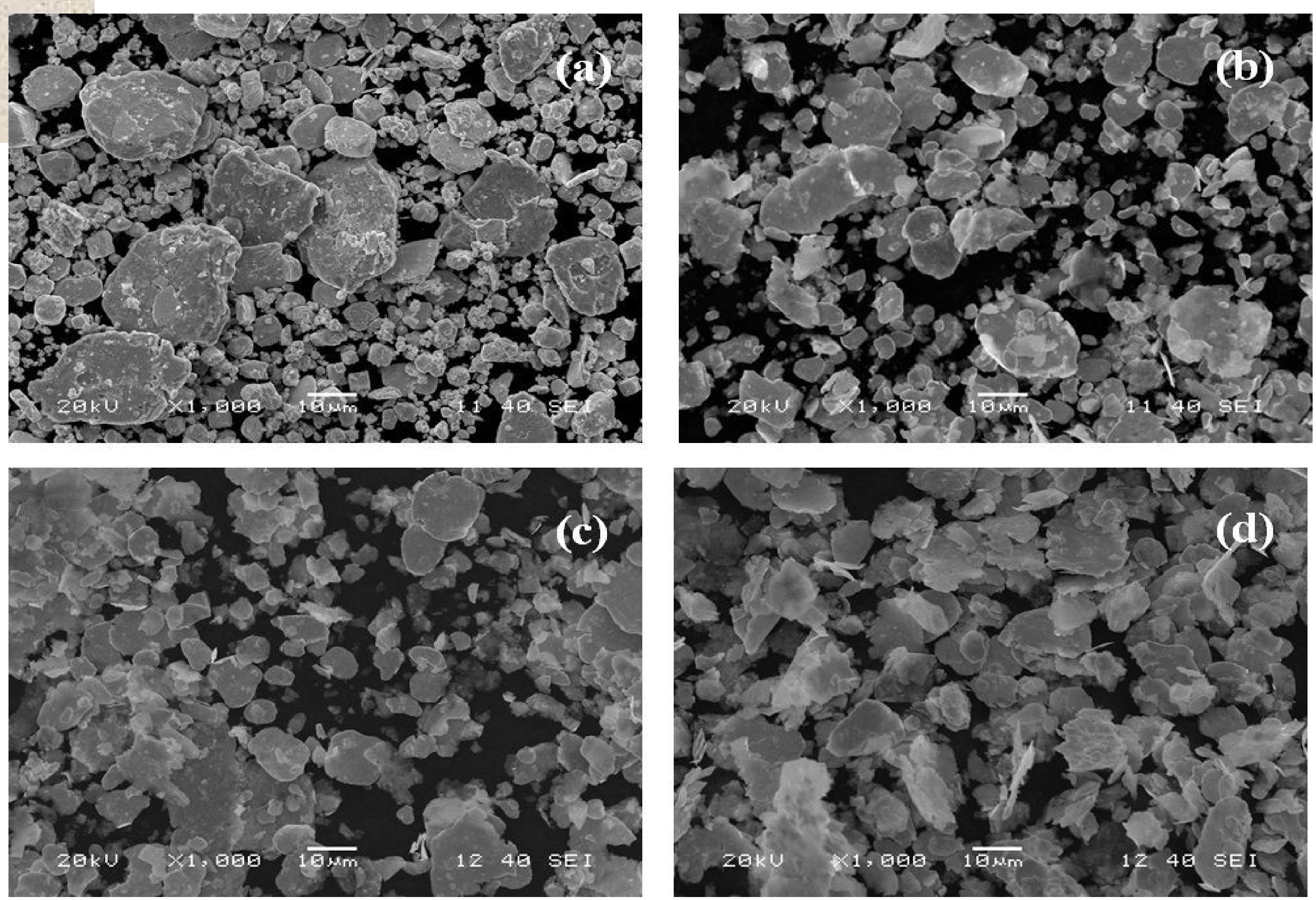

SEM micrograph of powder of alloy B at (a) 0 h, (b) 5 h, (c) 10 h and (d) 20 h of mechanical alloying.

Results and discussion

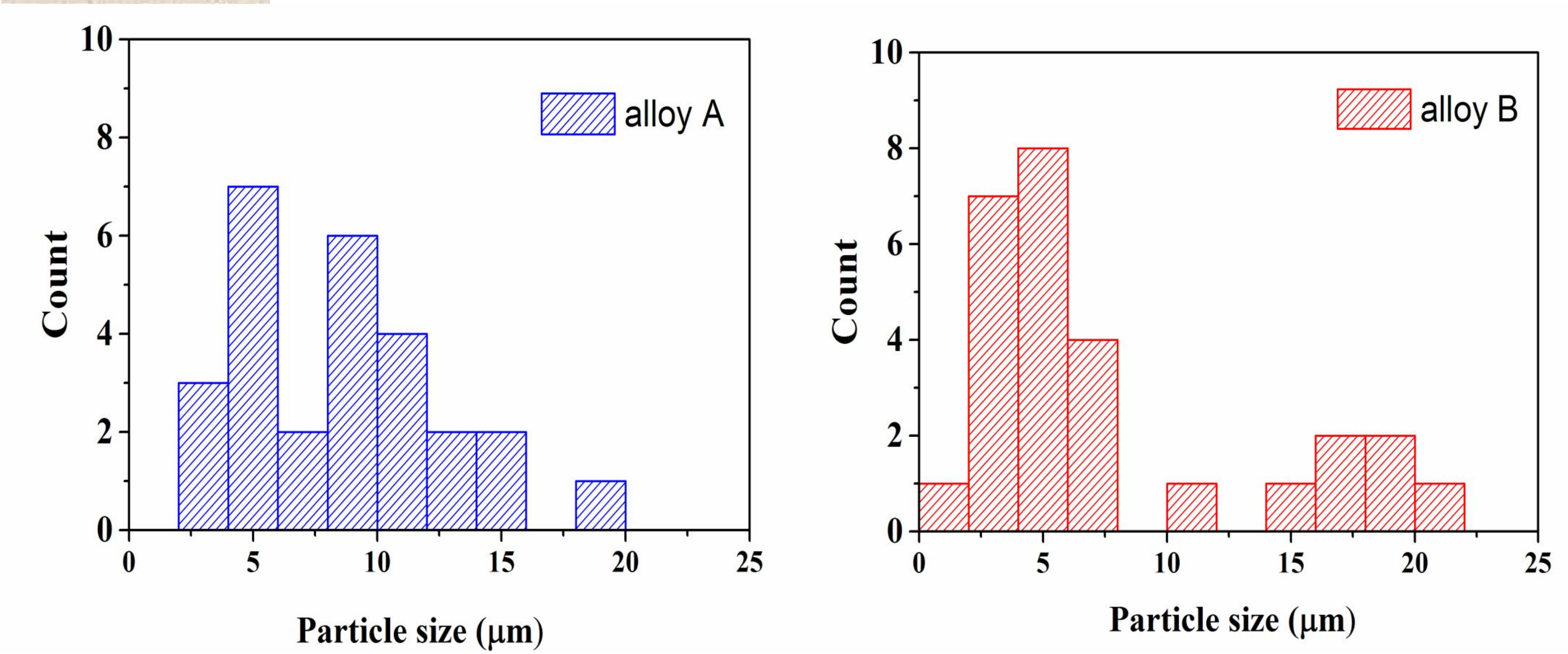

Particle size distribution of 20 h milled alloy A and alloy B.

Enhanced Bimodality represent superior particle packing during compaction.

Results and discussion

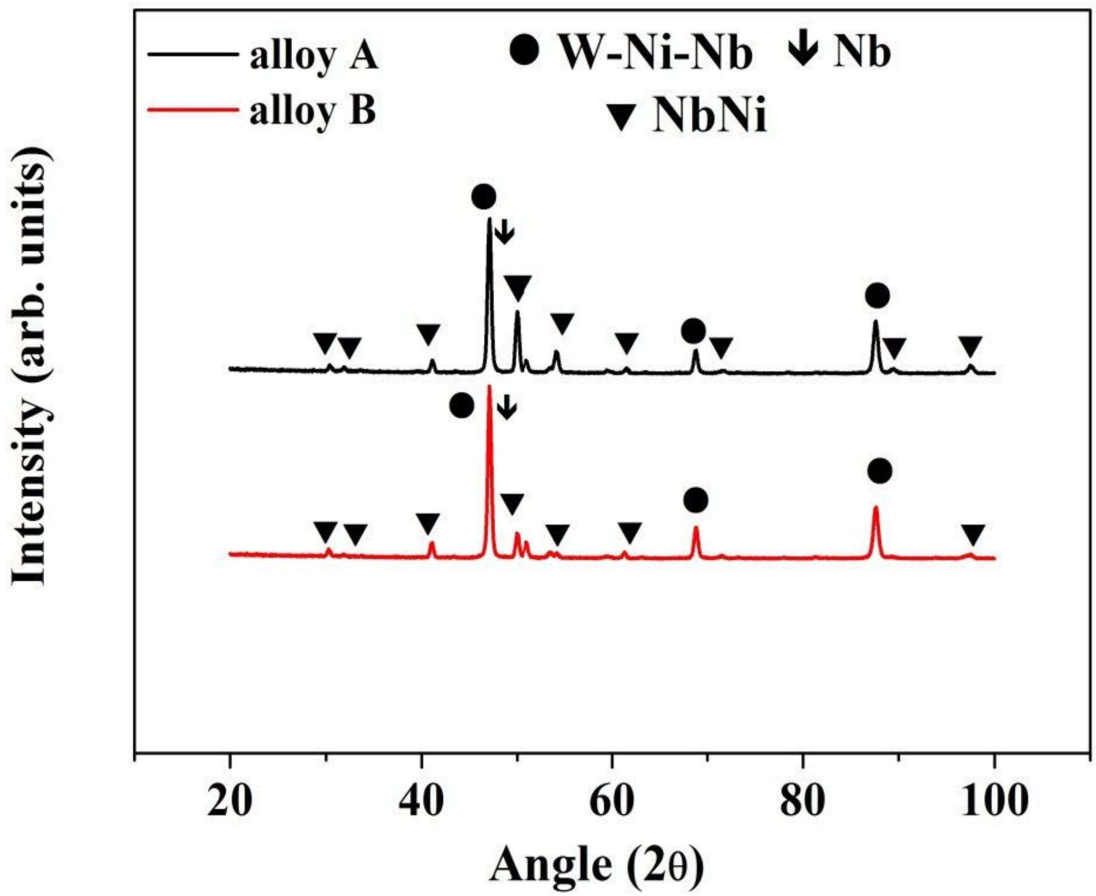

Peak Shift in (110) diffraction plane of 20 h milled W to higher angle in sintered alloys (alloy A: from 40.29° to 46.97°, alloy B: from 40.31° to 47.20°)

XRD pattern of alloy A and alloy B mechanically alloyed for 20 h and sintered at 1500°C for 2 h.

Results and discussion

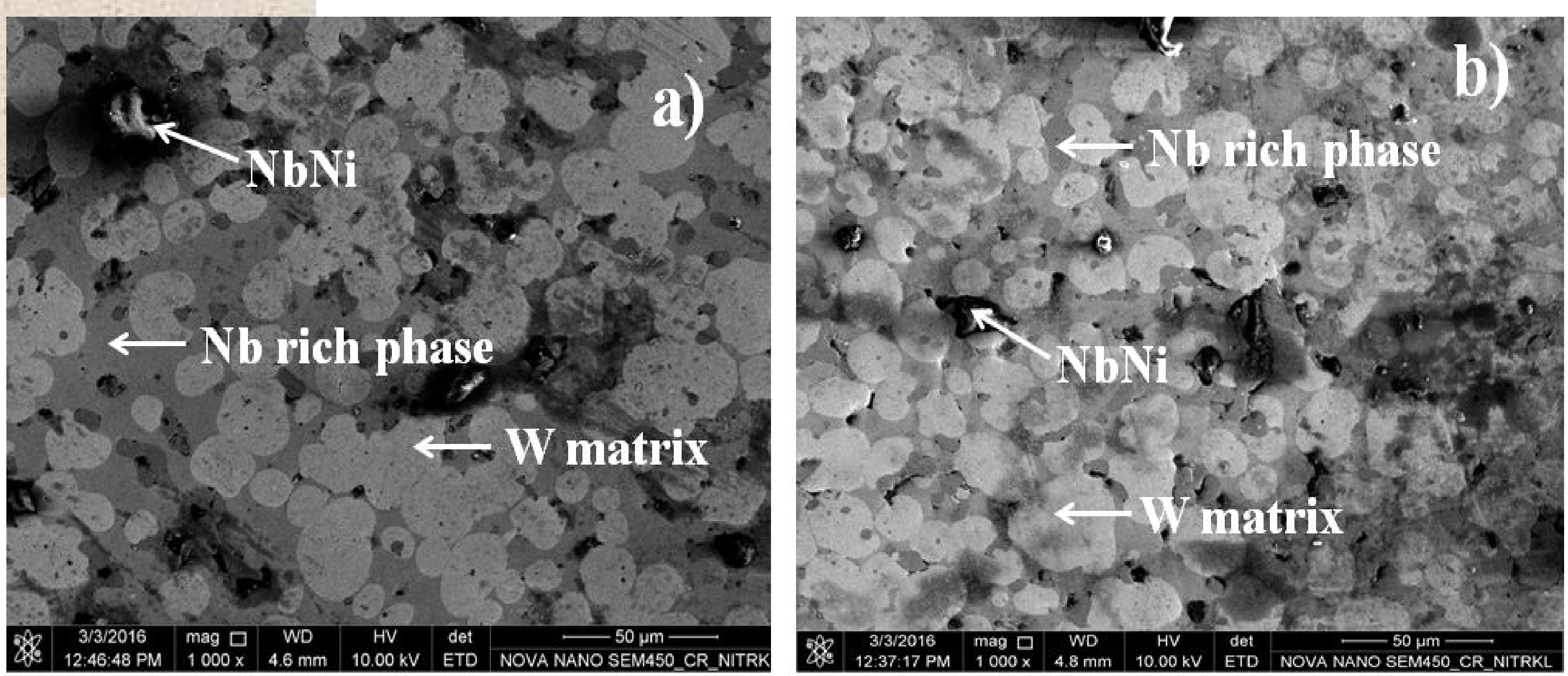

SEM micrograph of sintered (a) alloy A, (b) alloy B

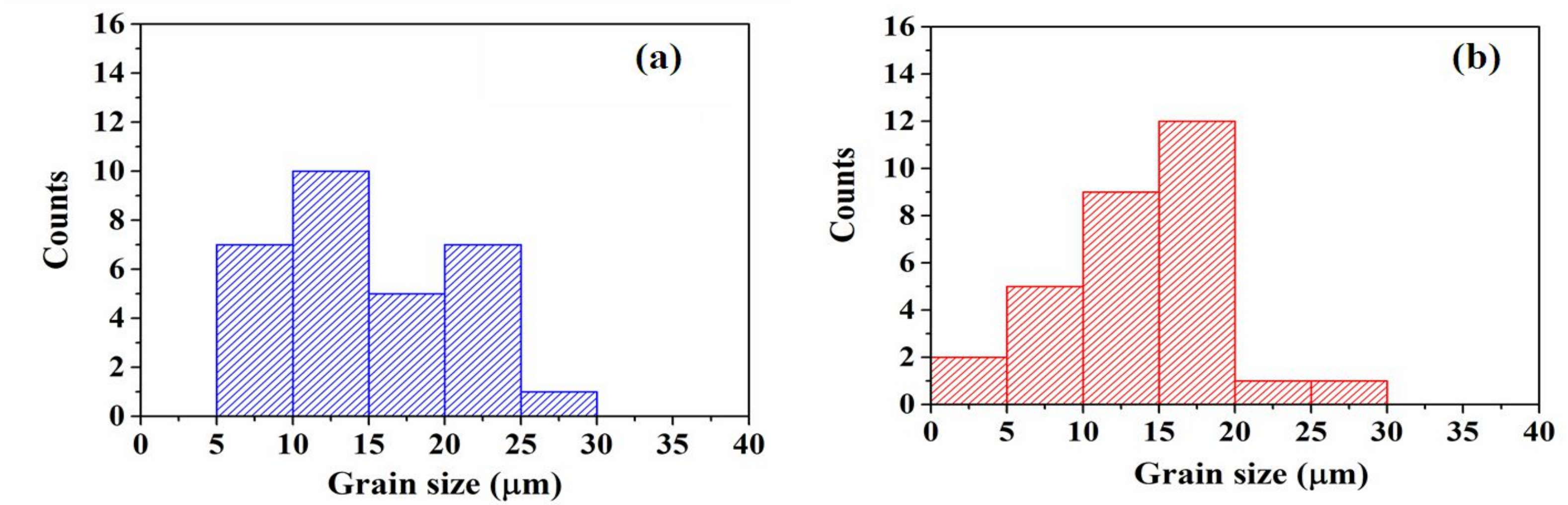

Histogram of sintered
(a) alloy A,
(b) alloy B

Results and discussion

$$\rho_s = \frac{W_a}{(W_{sat} - W_{susp})} \ X \ \rho_w \frac{gm}{cm^3}$$

W_a is weight of the sintered sample in air.
W_{sat} is the weight of the sample with all the open porosity saturated with water,
W_{susp} is the weight suspended in water. ρ_w is the density of water.

Alloy	Dry Weight (gm)	Soaked Weight (gm)	Suspended Weight (gm)	Theoretical Density (gm/cm^3)	Sintered Density (gm/cm^3)	%Sinterability
A	2.07	2.08	1.92	14.82	12.94	87.31
B	1.67	1.69	1.56	14.19	12.85	90.56

- **Superior particle bimodality in 20 h milled powder of alloy B.**
- **Low crystallite size → enhanced surface energy → improved mass transport**

Results and discussion

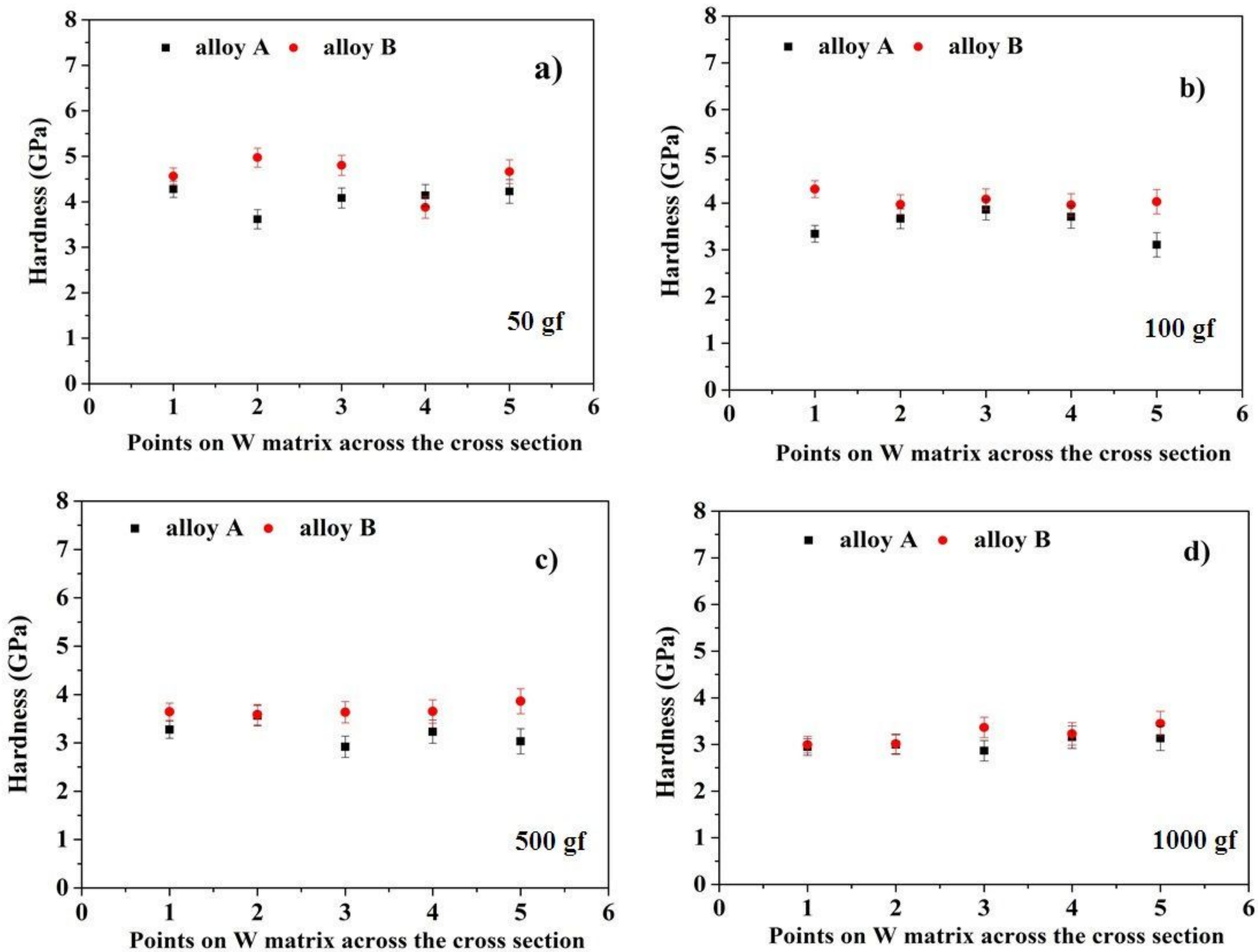

- **Enhanced density, Finer microstructure**
- **Smaller indentation at reduced loads (ISE)**
- **Stress field-dislocation core interaction**

$$\mathbf{HV} = \mathbf{1.8544}\,\frac{P}{d^2}$$

Results and discussion

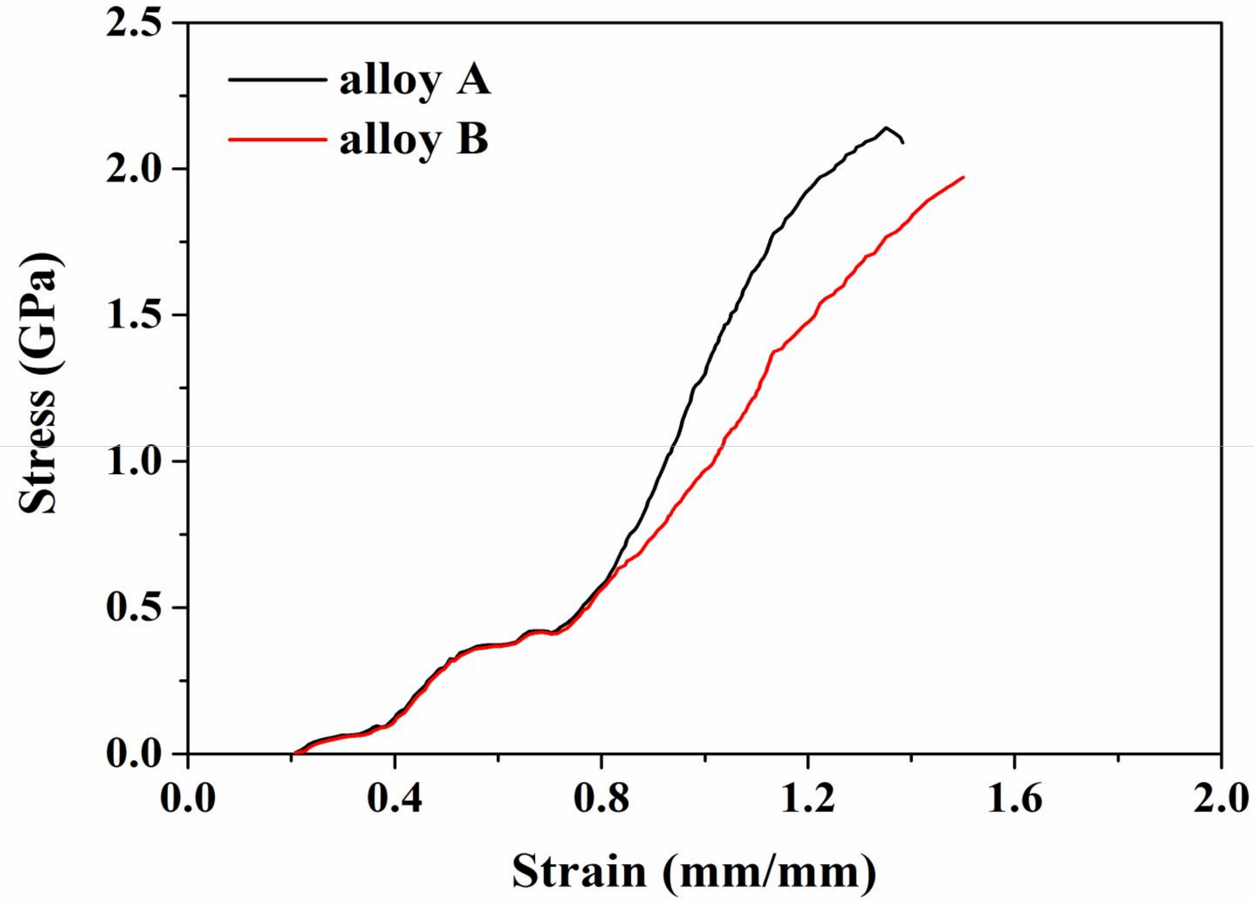

(strain rate: 10^{-1}/min)

- Higher hard brittle NbNi in alloy A. (high strength-low %strain to failure) than alloy A

True- stress- strain curve under Compressive loading

A. Patra et al. , Int. J. Refract. Met. Hard Mater 60 (2016) 131–146

Results and discussion

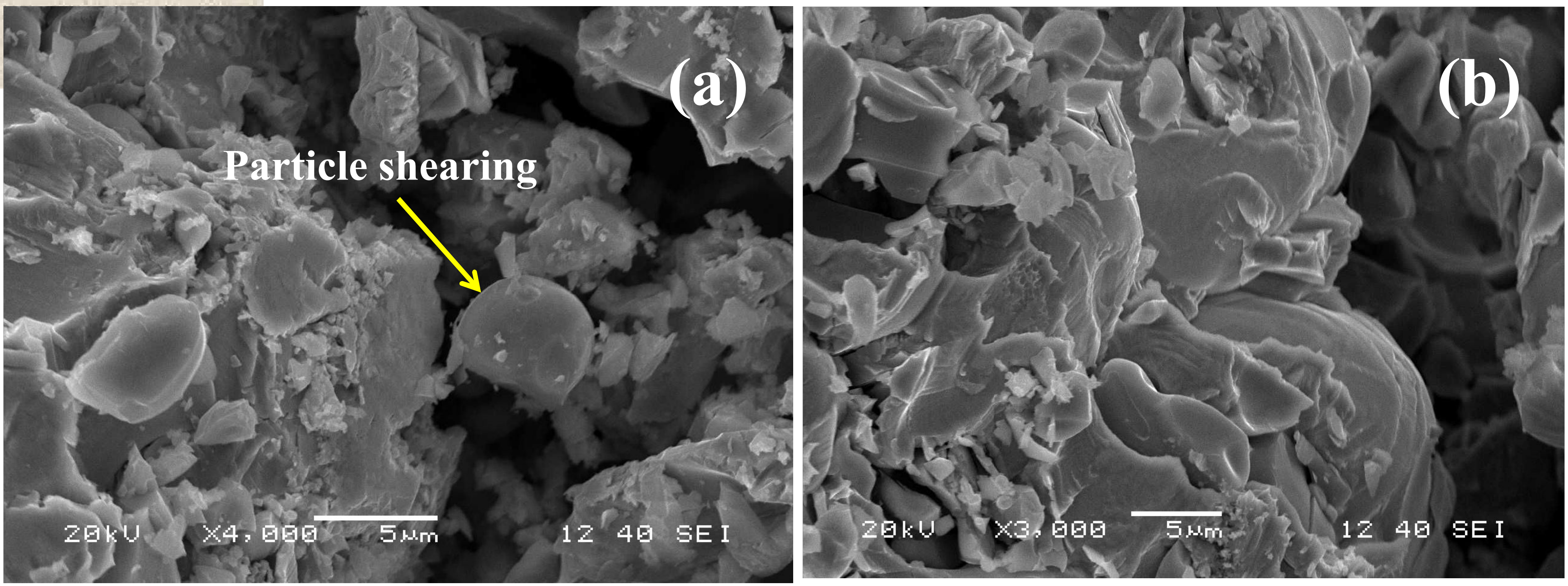

Fractographic study of (a) alloy A and (b) alloy B

Results and discussion

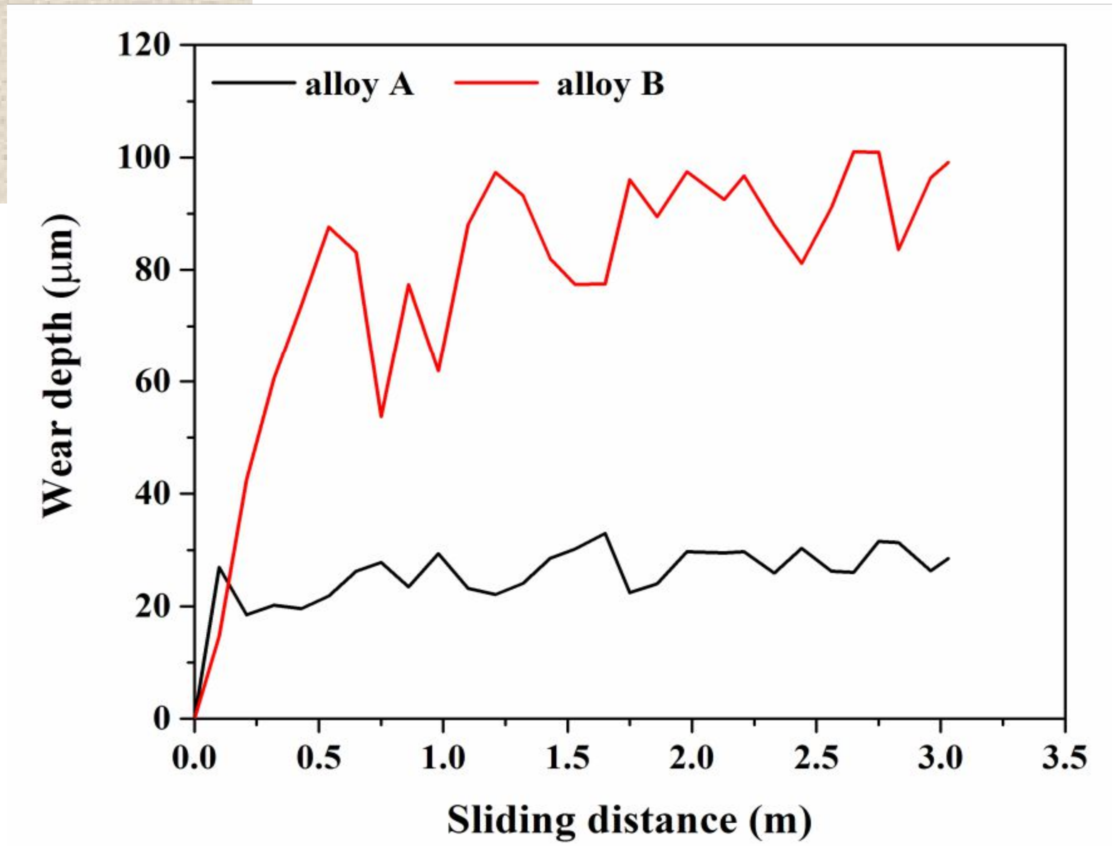

Higher fraction of hard NbNi particles strongly restrict the dislocation motion which results in lower wear depth in alloy A

$$\text{Sliding Distance (S.D)} = \left(\frac{\mathrm{N}}{60}\right) \times \mathrm{t} \times 2\pi\mathrm{r}$$

Test condition : 30 N load, 25 rpm, track diameter : 4 mm, time : 10 min.

Results and discussion

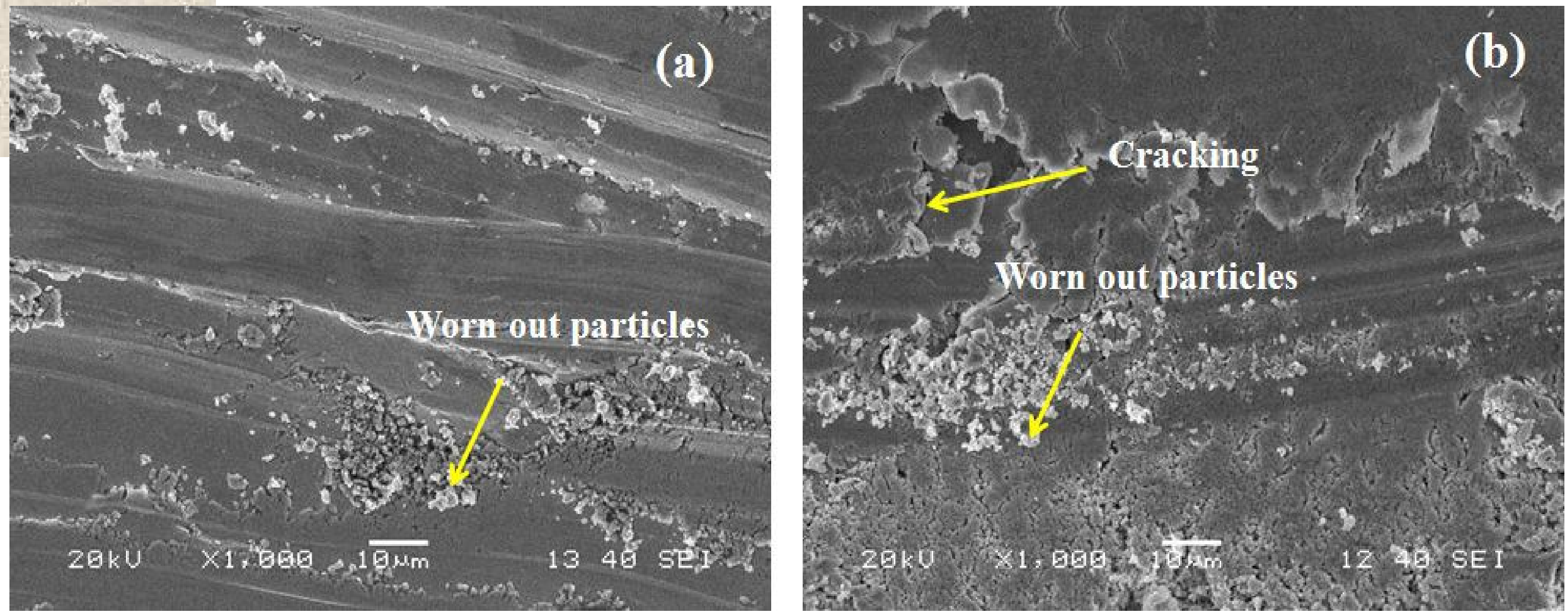

SEM micrograph of wear track of (a) alloy A, (b) alloy B milled for 20 h and sintered at 1500°C for 2 h at 30 N load.

Results and discussion

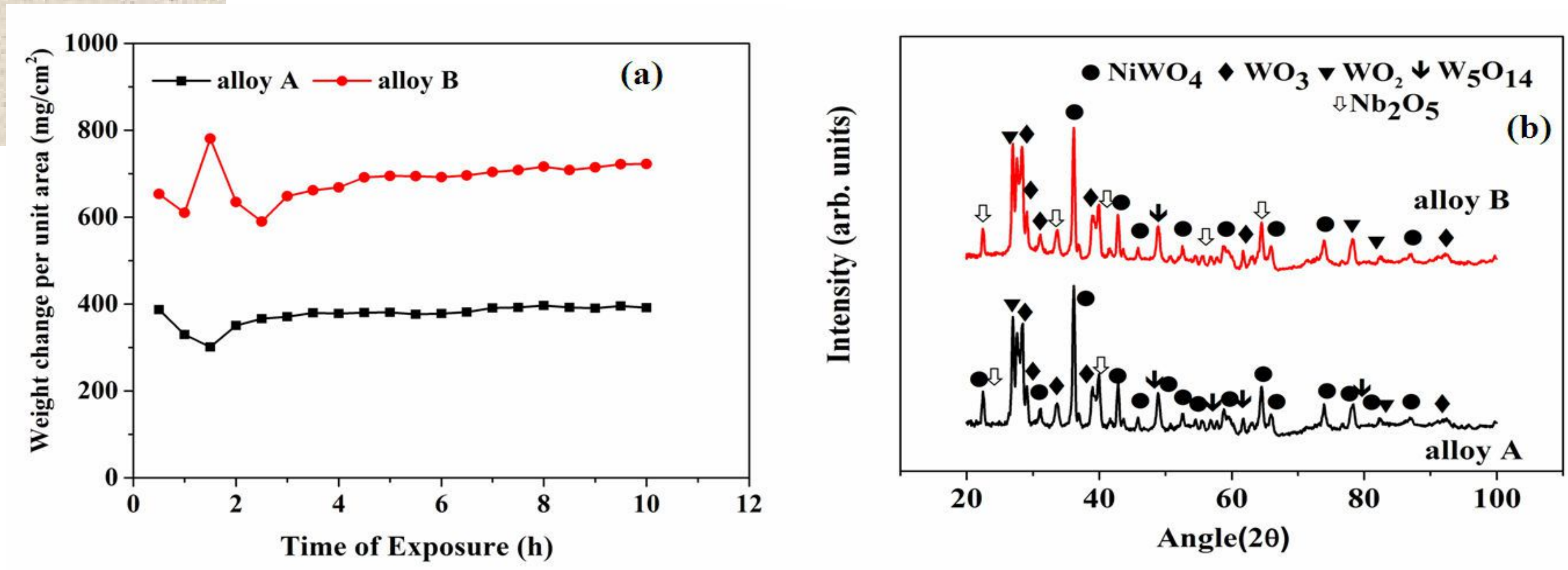

Weight change with exposure time of alloy A and alloy B during oxidation in furnace, (b) XRD pattern of alloys A and alloy B subjected to oxidation at 900°C for 10 h.

Results and discussion

$$\left(\frac{\Delta m}{A}\right)^2 = \mathrm{Kt} + \mathrm{C}$$

A. Patra et al. , Int. J. Refract. Met. Hard Mater 70 (2018) 134-154.

Oxides	ΔG_f° (KJ mol^{-1})
WO_3	- 349.3
Nb_2O_5	- 539.5
TiO_2	-688.69
NiO	-192.2

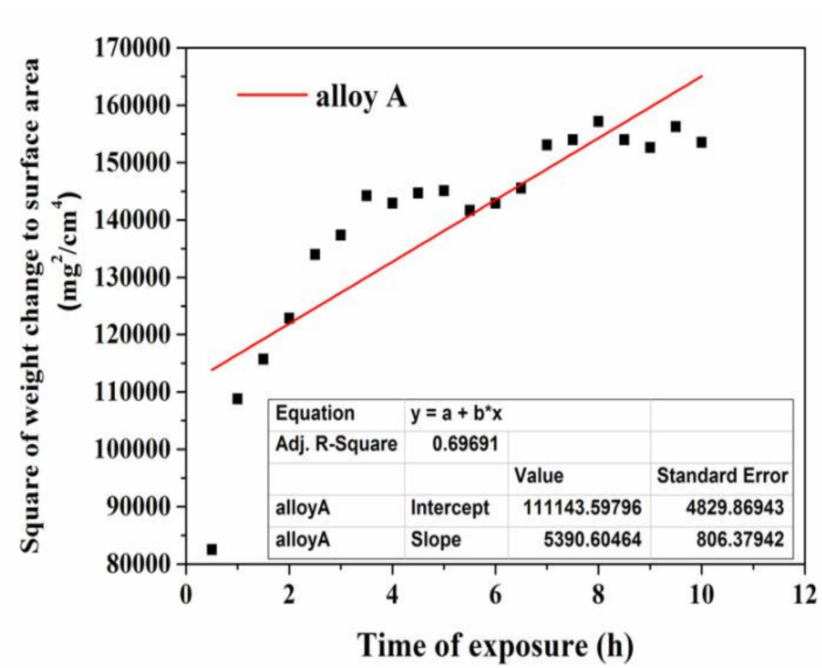

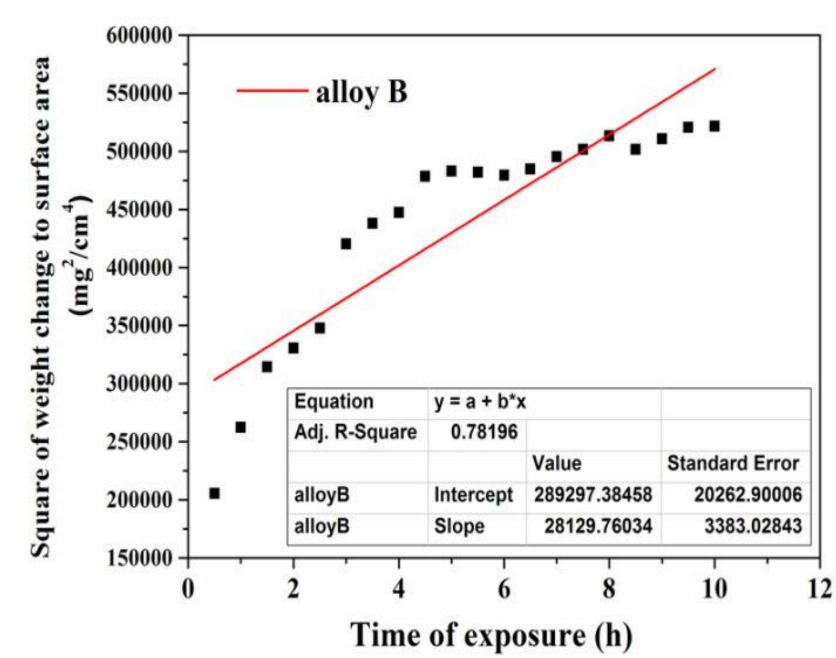

Molar volume of WO_3, WO_2, Nb_2O_5 is 31.76 cm^3, 19.57 cm^3 , 58.30 cm^3 respectively whereas the molar volume of impervious $NiWO_4$ is 38.56 cm^3

Conclusions

- **Nanostructured novel W-Ni-Nb alloy powders are produced by mechanical alloying. Minimum crystallite size of W and maximum lattice strain is achieved in $W_{75}Ni_{15}Nb_{10}$ alloy at 20 h of milling.**

- **The lattice parameter of W in all alloys expanded at 10 h of milling due to hydrostatic pressure exerted by the nanocrystals and contraction at 20 h of milling owing to formation of solid solution.**

- **Presence of NbNi intermetallic is evident in the sintered alloys due to Ni rich liquid phase formation at the selected sintering temperature.**

- **The % densification and hardness of $W_{75}Ni_{15}Nb_{10}$ alloy is higher as compared to $W_{70}Ni_{20}Nb_{10}$ alloy.**

- **$W_{70}Ni_{20}Nb_{10}$ shows higher strength and low % strain to failure as compared to $W_{75}Ni_{15}Nb_{10}$.**

Conclusions

- **Minimum wear depth is recorded in alloy A due to higher presence of NbNi intermetallic phase.**

- **High temperature oxidation behavior shows superior oxidation resistance of $W_{70}Ni_{20}Nb_{10}$ alloy as compared to $W_{75}Ni_{15}Nb_{10}$ due to lower W content and quick formation of more stable and impervious $NiWO_4$ oxide scale.**


Thank You!